Pinning of a single Abrikosov vortex in superconducting Nb thin films using artificially induced pinning sites

M. Breitwisch and D. K. Finnemore
Ames Laboratory, USDOE, and Department of Physics, Iowa State University, Ames, Iowa 50011
(Received 30 July 1999; revised manuscript received 9 February 2000)

Artificial structures were intentionally introduced into Nb films in order to study the interaction of a single Abrikosov vortex with pinning sites caused by these known defects. A vortex trapped on one of these structures or defects can be induced to move either by thermal depinning or by pushing on the vortex with a transport current in one of the films. The resulting motion, in turn, can be followed by observing the changes in the Fraunhofer-like interference pattern of a cross-strip Josephson junction having the thin film as one leg of the junction. Artificial pinning sites were successfully created by depositing Fe balls on the surface of a previously characterized thin film. Attempts to create artificial pinning sites by depressing the order parameter with a thin strip of Au on the surface of the Nb were not successful. There was no correlation between the location of trapped vortices and the location of the Au line. In a separate measurement, Lorentz-force-depinning studies for several intrinsic pinning sites in the thin film show that a transport current in the top film will depin a vortex in the top film with about one-tenth the current needed in the bottom film to depin the same vortex.

I. INTRODUCTION

Methods have been developed to nucleate a single Abrikosov vortex and systematically move it from place to place in a thin film.[1,2] So far, however, all the experiments have been done with the naturally occurring defects that develop as the film grows. Most of the earlier work strove to obtain films with very low pinning so that there would be a wide temperature window where the vortices would move easily. In this previous work, the basic principles were established to show that Josephson junction interference patterns can be used to specify the location of a vortex in a thin film,[2,3] and measurements of the elementary pinning force were made for a number on intrinsic pinning sites in both Pb and Nb thin films.[4,5] In addition, it was established that an intrinsically pinned vortex will spontaneously start to move around when the superconducting order parameter Δ is suppressed to about 20% of the $T=0$ value Δ_0.[1,6,7] In all of this work, there was no control of the locations where the vortex would move.

The goal of this work is to study the interaction between a single vortex and a known defect that induces pinning. To use the motion of a single vortex either for basic physics studies or in a device, it is important to develop ways to guide the trajectory of the vortex in the thin film by creating artificial structures either in or on the thin film. It is useful to know which materials work effectively and to measure the resulting forces in some detail. It is also important to explore quantitatively the the most effective way to apply forces to the vortex in any desired direction. More specifically, effectiveness of both direct currents and induced currents as methods to apply a force to the vortex should be understood quantitatively. Thermal depinning is an essential measurement in this work to specify unambiguously the film in which the vortex resides and the response of the superconducting order parameter to the artificial pinning material. In this work we use both Fe and Au defects on the thin film and measure the elementary pinning forces. In addition, we explore the relative effectiveness of using both direct current and induced currents to push on a vortex pinned at the same location. Induced currents in a film have current density patterns that are different from direct currents, so it is important to use both kinds of currents to study pinning from several different kinds of pinning site.

With the development of methods to nucleate a single Abrikosov vortex in a superconducting thin film and systematically move it from place to place,[8] it has become possible to carry out fundamental studies related to the use of a single Abrikosov vortex as a logic or memory element. For example, it is now possible to measure the elementary pinning force holding an Abrikosov vortex on a variety of different naturally occurring and artificial pinning sites. In addition, studies can be made of the physics involved in different methods to apply a force to a vortex to move it from one location to another. If a force is to be applied in any desired direction, both direct currents along a film and induced currents across the film must be used. The direct current pushes the vortex perpendicular to the axis of the film and the induced current pushes the vortex parallel to the axis of the film. Our goal in this work is to study both the magnitude of the pinning force as well as the method to apply the force. Two different ways to pin a vortex at a specified location are studied, first by locating an Fe ball on the surface, and second by dumping electrons into the superconducting thin film from an adjacent Au line. Studies are then made of thermal depinning to determine the temperature where a vortex will spontaneously depin and move with no applied force as well as studies of the relative efficacy of direct and induced currents to apply a Lorentz force to the vortex in the film. Taken together, these experiments are all related to the problem of nucleating and systematically moving a vortex through a series of specified locations.

To create an artificial pinning site in a superconducting

thin film, it is necessary to introduce a defect that creates a space dependence in the superconducting order parameter at a specific location. In this work, two different types of artificial defects were used. First, ferromagnetic particles Fe were placed on top of the junction region of the thin film. The effect of the Fe ball is twofold. The magnetization of the Fe creates a magnetic field in the Nb and in addition, normal electrons from the Fe can flow into the Nb, thus lowering the superconducting pair potential by the proximity effect. This dip in the pair potential can pin a vortex at that location.

A second method to form an artificial pinning site was to deposit a narrow stripe of Au on the Si substrate[1] and then deposit a Nb film over the Au stripe. Normal electrons from the Au will flow into the Nb, suppressing the order parameter within a coherence distance of the point of contact to form a line pin. A vortex within the Nb film will have a lower energy residing above the Au line than elsewhere in the film.

To conduct these experiments, it is necessary to determine the location of a single vortex and to follow its displacement as it moves around the thin film. This is done by incorporating the thin film into a cross-strip Josephson junction and measuring the Fraunhofer-like interference pattern for the critical current vs magnetic field applied parallel to the junction, I_c vs B_y.[1,2] A magnetic field parallel to the plane of the junction modulates the relative phase between the two superconducting films to produce a diffraction pattern. With no vortex in the junction, the classic Fraunhofer pattern is seen for a plot of the junction I_c vs B_y. When a vortex penetrates one of the films in the cross-strip junction region and leaks out through the normal Ag-Al barrier to the edge of the junction it acts as a source or sink of magnetic flux, altering the I_c vs B_y pattern. There is a direct correlation between the location of the vortex and the shape of the interference pattern so that the interference pattern can be used as a ''finger print'' to specify the location of the vortex.[2] As reported previously, a vortex near the center of the junction gives a two peak structure with a minimum in I_c at $B_y=0$.[2] A vortex near the edge of the junction gives a pattern only slightly different from the Fraunhofer pattern.

II. EXPERIMENTAL TECHNIQUE

Cross-strip superconductor-normal-insulator-superconductor (SNIS) Josephson junctions were prepared in a three-gun sputtering system. Typically, the chamber was evacuated to about 1.5×10^{-6} Pa and back-filled with the desired pressure of Ar, $\sim$20 mTorr. A load-lock mechanism was available so the substrate could be lifted to change masks without breaking vacuum. First, a strip of Nb was sputtered onto the oxidized Si substrate about 100 μm wide and 400 nm thick for the bottom Nb film. A Ag strip about 150 nm thick was deposited over the bottom Nb strip using the same mask to provide a normal metal barrier and to protect the bottom strip during the Al oxidation step. An Al strip, substantially wider than the Nb and Ag bottom strip, was deposited over the Ag to a thickness of about 350 nm. At this point Ag pads for electrical contacts were sputtered onto the Si substrate and the edges of the Al layer to make good contact with the Al before it was oxidized.

Two different oxidation methods were used to oxidize the Al. For the first sample, a negative voltage of 512 V was applied to an Al ring below the substrate and about 80 mTorr of oxygen was admitted to create a glow discharge for one hour. For the second and third samples, the Al layers were oxidized by exposing them to air for one minute. After the oxidation process, the pressure was reduced below 2×10^{-6} Pa and the Ar pressure was brought to about 20 mTorr. A top Nb strip that was 100 μm wide, 400 nm thick, and oriented perpendicular to the bottom strip was then deposited. For the second and third samples, collimators were added to the Nb sputtering masks to reduce shadowing effects. This resulted in the Nb strips of these junctions to be much narrower, approximately 55 μm.

The superconducting transition temperatures of the Nb films for samples 2 and 3 are lower than those for the Nb films of sample 1 despite similar preparation methods. Despite the lower T_c values, the junctions for samples 2 and 3 were perfectly satisfactory for nucleating single vortices and following the motion with the diffraction pattern method.

Electro-expanded Fe balls in a hexane solution were obtained from The Argonide Corp. of Sanford, FL. The individual particles of Fe are nearly spherical with radius approximately 50 to 100 nm. To break apart the larger clumps of Fe particles the solution was placed in an ultrasonic cleaner before a drop of solution was extracted and placed on top of the junction region. The drop of hexane would evaporate within a few seconds leaving behind Fe particles and a thin residue on top of the surface of Nb. Two Fe balls, approximately 10 μm in diameter, were successfully placed on top of the junction region. No direct measurements were made of the internal structure of the Fe balls but they could be aggregates of hundreds of smaller balls.

Samples designed to use Au lines as pinning centers were fabricated on Si substrate that had an array of Au lines on it. An oxidized Si wafer was coated with 10 nm of Ti followed by 20 nm of Au in a parallel array 2 μm wide spaced 60 μm apart using standard photolithography techniques. The function of the Ti is to provide a buffer to give a better sticking coefficient for the Au. An array of Au lines was needed because the placement of the Nb films relative to a single Au line is not sufficiently precise. Other details of the measurements are the same as discussed previously.[8]

III. RESULTS AND DISCUSSION

A. Fe balls on top of sample 1

A full characterization of the Josephson junction was done before the Fe balls were deposited, and some of the characteristics of this junction are reported elsewhere.[8] The main features of this junction are the transition temperatures of each film, 9.310 and 9.056 K for the top and bottom Nb films, respectively. The oxidation of the Al always seems to degrade the T_c of the bottom film, presumably because some oxygen gets into the bottom Nb layer even though it is coated with both Ag and Al. All diffraction patterns were measured on this sample at 8.416 K, a temperature where we are in the small junction limit. Iron balls were placed on top of this already characterized Josephson junction so that the intrinsic pinning sites would not be mistaken for the artificially induced pinning sites.

Figure 1 shows the scanning electron microscope (SEM) micrograph of sample 1. The focus of the microscope is set

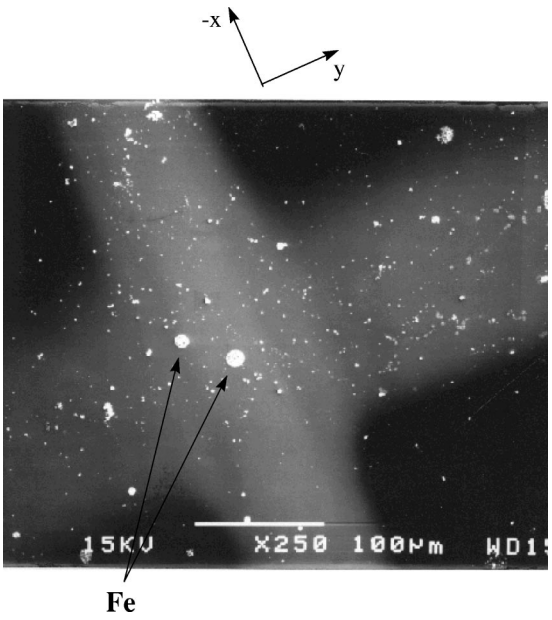

FIG. 1. SEM micrograph of sample 1 with two Fe balls on top of the junction region where the two Nb films cross. The top film is along the *x* direction. The other particles in the photo contain no Fe and are dust residue from the processing and transport of the sample.

to highlight the $5-10$ μm diameter Fe balls. The bottom film is along the *y* axis. The bottom film also appears wider than the top film because the bottom Nb film is covered with a layer of Al that is wider than the Nb film itself. The edges of the films appear rather fuzzy and not well defined. This is due to microscope focus and shadowing effects which occurred during sample preparation. The shadow mask for the Ag and Al depositions was raised to guarantee wider normal metal overlays and this gives more tapered edges for the normal metal parts of the film.

Energy dispersive spectroscopy (EDS) was used to check the composition of all the visible particles on top of the junction region. The two largest balls with (x,y) coordinates $(-0.05,-0.05)$ and $(-0.80,-0.75)$ in units of $W/2$, where W is the width of the junction, were determined to be Fe. These are only approximate coordinates as the junction region shown in Fig. 1 does not appear to be well defined. The other particles were determined to be dust. This dust came from the sample being exposed to air during the transfer of the sample from the sputtering chamber to the cryostat, from taking the sample out of the cryostat to place Fe balls on top of the junction, and from transporting the sample from the cryostat to the SEM.

Before the addition of the Fe balls, cooling through T_c with current up to 0.35 mA through the top Nb film would not nucleate vortices. After the addition of the Fe balls, one of two diffraction patterns would be obtained upon zero-field cooling as shown in Figs. 2(a) and 2(b). The diffraction pattern in Fig. 2(a) matches very well with the theoretical curve for a positive vortex at $(-0.05,-0.05)$. Similarly, the diffraction pattern shown in Fig. 2(b) matches well with the theoretical curve for a positive vortex at $(-0.80,-0.75)$. The net magnetic moments of the Fe balls were strong enough to nucleate vortices and act as artificial pinning sites.

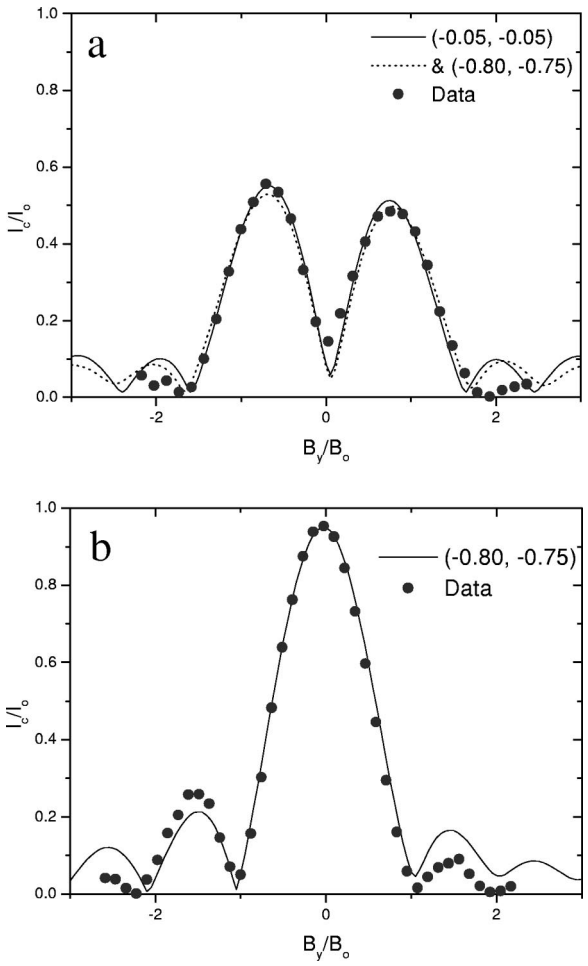

FIG. 2. Vortices pinned beneath the two Fe balls resulted in diffraction patterns (circles) which match the theoretical patterns (lines) for single vortices at the locations of the Fe balls as determined by SEM measurements. (a) Single vortex at $(-0.05,-0.05)$ and (b) single vortex at $(-0.80,-0.75)$.

Once these two pinning sites were discovered, the next step was to characterize them with thermal and current depinning experiments. Starting with a vortex which was pinned on the central Fe ball, the temperature was raised in intervals of 3 mK to determine the temperature at which the vortex would thermally depin. The data taking sequence was to warm to a specified temperature, cool to $T_{\text{measure}} = 8.416$ K, and measure an V vs I curve to see if the vortex has moved. If the vortex had moved, a full diffraction pattern was taken to find the new location. It is important to point out that it is difficult to distinguish between a one vortex pattern with the vortex at $(-0.05,-0.05)$, and a two vortex pattern with one vortex at $(-0.05,-0.05)$ and a second vortex at $(-0.80,-0.75)$. This is illustrated in Fig. 2(a) where the solid line is a model fit with just one vortex at $(-0.05,-0.05)$ and the dotted curve is a model fit with one vortex at $(-0.05,-0.05)$ and a second vortex at $(-0.80,-0.75)$.

As the temperature was increased the initial diffraction pattern changed slightly, indicating small movements of the vortex beneath the Fe ball. At a temperature of 9.145 K the diffraction pattern changed shape drastically from Fig. 2(a) to Fig. 2(b), indicating that the vortex depinned and moved

to the second Fe ball. Upon raising the temperature higher in steps of 3 mK, something rather unexpected occurred; the pattern changed back and forth between the pattern of Figs. 2(a) and 2(b). This continues all the way from 9.145 to 9.531 K. The interpretation is that either (1) a single vortex hops back and forth between the two Fe balls or (2) there always is a vortex on the Fe ball near the edge and the vortex on the Fe ball near the center is sometimes there and sometimes exits the junction. In this thermal depinning sequence, the only two patterns observed were Fig. 2(a) and 2(b).

Next, Lorentz force depinning experiments were performed with a vortex initially pinned beneath the central Fe ball in order to determine the pinning force of this artificially induced pinning site. To take a data point, the temperature is raised to a set temperature to be used for Lorentz depinning, a push current was applied in the top film for 1.0 *s* and turned off. Then the junction temperture was changed to 8.416 K where an I_c vs B_y curve was taken to see if the vortex had moved. If it had not moved, the process was repeated at successively higher push currents until the vortex moved. Using increments of 0.50 mA, the vortex depinned at a push current of 6.5 mA and moved to the location of the second Fe ball. When the current was then increased to 7.5 mA, the resulting diffraction pattern began to deviate from a one-vortex pattern, indicating more vortices on the edge of the film had been nucleated.

In order to find the depinning current more precisely, the experiment was repeated beginning with $I_{\mathrm{push}}=6.0$ mA using increments of 0.1 mA. The results are shown in Fig. 3. At 6.2 mA the vortex began moving around underneath the Fe ball in a path uncorrelated with the direction of the Lorentz force on the vortex. This continued until 7.4 mA at which point the vortex depinned from the Fe ball and moved in the negative *y* direction as shown in Fig. 3. A current of 7.9 mA pushed the vortex further in the negative *y* direction. This motion is consistent with the direction of the Lorentz force on a positive vortex produced by a positive current in the same film as the vortex. A larger current of 8.0 mA then pushed the vortex to the position of the second Fe ball.

The minimum depinning current of 7.4 mA at a reduced temperature $T/T_c=0.9$ can be related to the pinning force of the Fe ball. The Lorentz force per unit length on a vortex from current density **J** is given by $\mathbf{J}\times\mathbf{\Phi}_0/c$. When the penetration length $<$ film thickness $<$ width, in a thin film, the current per unit width can be written as $I'=(I/\pi)/[(W/2)^2-x^2]^{1/2}$, where *x* is the measured distance from the center of the film. Combining these results gives a pinning force of 9.8×10^{-14} N.

An estimate of the total magnetic moment of the central Fe ball can be made by examination of the thermal depinning and current depinning results. The thermal energy required to depin a vortex pinned on the central Fe ball, kT, can be compared with the magnetic energy gained from the vortex aligning with the magnetic moment of the Fe ball $\mu_{Fe}\cdot\mathbf{H}_{\mathrm{vortex}}$. For $T/T_c=0.98$ where thermal depinning occurs, $\mathbf{H}_{\mathrm{vortex}}=0.004T$, this comparison yields a result of $\mu_{\mathrm{Fe}}\sim3.5\times10^{-20}$ J/T. Also, for Lorentz force depinning at $T/T_c=0.90$, the force between a magnetic particle and a vortex,[9] $(\mu_{\mathrm{Fe}}\Phi_0)/(2\pi\lambda^2\xi)$, where λ is the penetration depth and ξ is the coherence length, can be compared to the measured depinning force 10^{-13} N. Using $\lambda\sim\xi\sim120$ nm, this comparison yields the result $\mu_{\mathrm{Fe}}\sim6.2\times10^{-19}$ J/T. These two estimates of μ_{Fe} differ by more than a factor of 10, but this close to T_c, that may be as close as the variables can be estimated. If the central Fe ball would have been one single domain, its net magnetic moment would have been 7.2×10^{-11} J/T. This implies that the central Fe ball is divided into many domains with random orientations yielding a very small net magnetic moment. Furthermore, the directions of the magnetization of the Fe balls can not be determined although they appear to have some component along the negative *z* axis since positive vortices were nucleated.

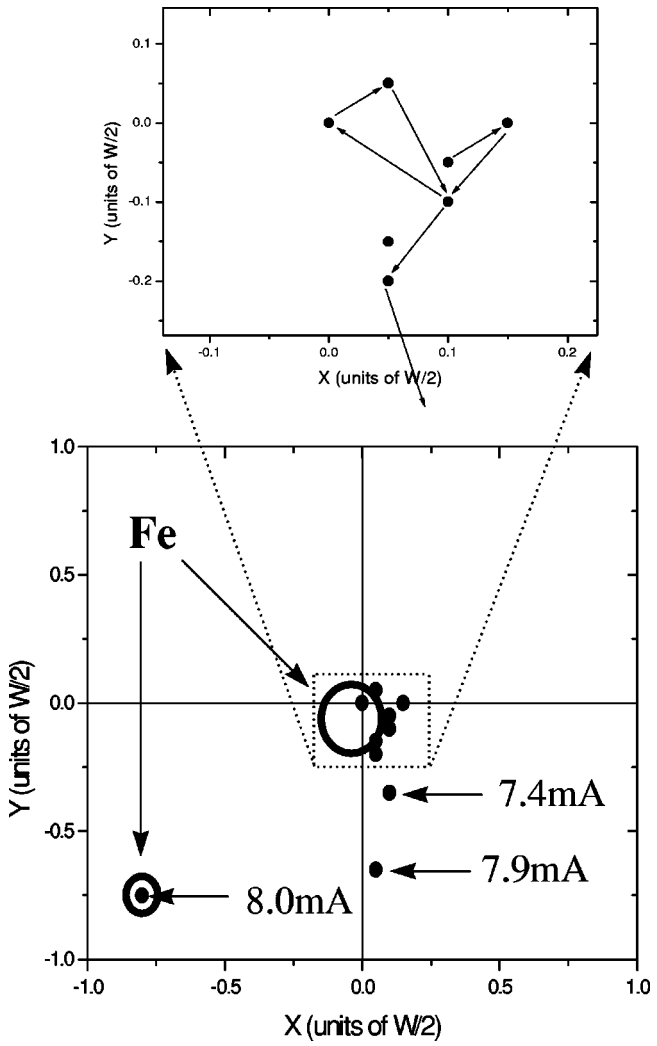

FIG. 3. Lorentz force depinning experiment with vortex initially pinned beneath the central Fe ball. A transport current of 7.4 mA through the top Nb film depinned the vortex from the Fe ball.

B. Sample 2—with a Au line

One of the junctions was prepared with a Au line adjacent to the bottom Nb strip in order to try to create an artificial pinning site along the line. Presumably, normal electrons would travel from the Au into the Nb and thus lower the superconducting pair potential in the region of the Au. The Au line is adjacent to the Si substrate and runs along the *x* direction in the lower half of the junction region at about $y=-0.36$ in units of the junction half width as illustrated in the SEM micrograph of sample 2 in Fig. 4.

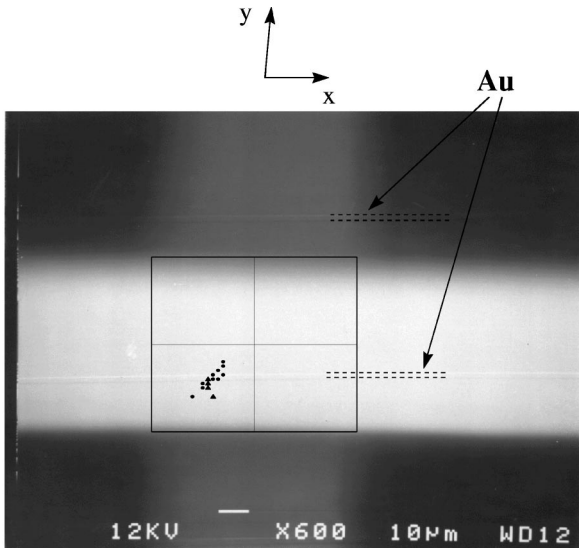

FIG. 4. SEM micrograph of sample 2 showing the location of the Au line beneath the junction. The top Nb film runs along the x direction. Also shown are the locations of all vortex pinning sites observed in the bottom Nb film.

Because the Au line was adjacent to the bottom film, it is important to be able to systematically nucleate a vortex in that film. To do this, we used the fact that the bottom film has a lower T_c than the top film. To nucleate a vortex in the bottom film the junction was stabilized between the T_cs of the two films. At this temperature the top film is superconducting and acts as a ground plane, screening any magnetic field from its interior. A current was then applied in the bottom film and the heater was turned off dropping the temperature to 4.2 K. This process traps a vortex in the bottom film. To nucleate vortices in the top films, the junction was warmed above T_c of both films and then allowed to cool with either a transport current in the top film or an applied magnetic field oriented perpendicular to the junction. For vortices nucleated in this manner, the vortex thermally depinned at temperatures above T_c of the bottom film, indicating that the vortex was in the top film.

If the Au underlay were to form a strong pinning site, one would expect that vortices in the bottom film would nucleate on the Au. They do not. The four different initial nucleation sites that were obtained are shown by solid triangles in Fig. 4. Most of the time, the vortex nucleates at $(-0.45,-0.50)$ and the Au line is located at $y=-0.36$. The other location that were sometimes obtained are indicated by triangles in Fig. 4.

Starting with a vortex at $(-0.45,-0.50)$, in the bottom film, thermal depinning experiments were carried out to see if the vortex would move to a line that we could later identify as the Au line by SEM. It did not. Using a temperature increment of 3 mK, a thermal depinning sequence showed that the vortex nearly always exited the junction on the initial thermal depin at 8.264 K. If the vortex did not exit, it moved to one of the sites shown by solid dots in Fig. 4.

Next, current depinning experiments were attempted. At 7.892 K a vortex at (0.045, 0.50) was successfully pushed to many other locations without nucleating more vortices. The locations of all the pinning sites observed are shown by the solid dots in Fig. 4. Since the polarities of the vortices were not known, the locations could have been those shown in the figure or those generated by reflections about the x and y axes. The pinning sites seem to be clustered around the line $y=x$. Because the Au line runs in the x direction, the pinning is probably not due to the proximity effect from the Au. Although a few of the pinning sites may lie on top of the Au line, the pinning sites span a large region of the junction. There does not appear to be any correlation between pinning and the presence of the Au line. The absence of pinning on the Au line may arise because the Au tapers over a distance much larger than the coherence distance so that the force is small even though the energy difference is fairly large.

A third junction with very similar characteristics to those of sample 2 was deposited on top of another strip of Au which ran along the y direction. Only four pinning sites were obtained in the bottom Nb film of sample 3 using the same current-nucleation methods discussed previously. None of them were located close to the Au line.

C. Intrinsic pinning sites in the top Nb film of sample 2

A rather different method was developed to nucleate a single vortex in the top film: the temperature was stabilized at 8.440 K, a field of 405 mG was applied perpendicular to the face of the junction, and then the temperature was dropped to 4.2 K. Using this nucleation method, four different pinning sites where obtained in the top Nb film. As stated previously, it is known that they are in the top film because vortices pinned at these sites thermally depin above T_c of the bottom Nb film. The amount of data that could be obtained for each pinning site was determined by the frequency with which a vortex appeared on that site.

A fairly extensive study of the anisotropy of the pinning potential was undertaken for vortices trapped in this top film. By applying currents in different films, a vortex can be pushed in different directions[5,6] and information about the symmetry of the pinning potential can be obtained. An applied current in the bottom film will induce screening currents in the bottom of the top film with equal magnitude and opposite direction.[5,6] For all four pinning sites, applied current through the bottom film would nucleate vortices before depinning the central vortex for temperatures below T_c of the bottom Nb film. At 8.292 K and higher temperatures, however, the vortex could be depinned with a transport current through either Nb film before any further nucleation would occur.

The first pinning site studied has a location of $(0.00, -0.20)$. Twenty one diffraction patterns for this site showed a scatter of only a few percent in the coordinates of this location. Out of the twenty-one times vortices depinned from $(0.00,-0.20)$, there were only two times that the vortex, upon depinning, did not hop to the position $(0.65,-0.10)$, regardless of the direction of the Lorentz force on the vortex. A vortex pinned at $(0.00,-0.20)$ thermally depinned at 8.431 K and hopped to $(0.65,-0.10)$. Figure 5 shows the current at which the vortices located at $(0.00,-0.20)$ first depinned for currents in the top (I_T) and bottom (I_B) Nb films. The only function of the connecting lines in Fig. 5 is to group together the data from current-depinning experiments performed at the same T_{push}. At a $T_{\mathrm{push}}=8.392$ K, 24.0 and -24.0 mA applied through the bottom film was required to

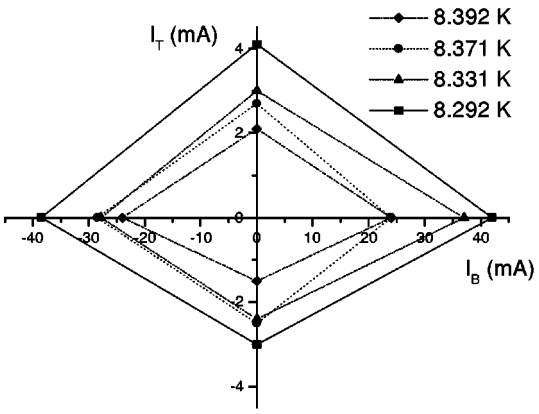

FIG. 5. Minimum depinning current for vortex pinned as in (a) for current applied through the top (ordinate) and bottom (abscissa) films.

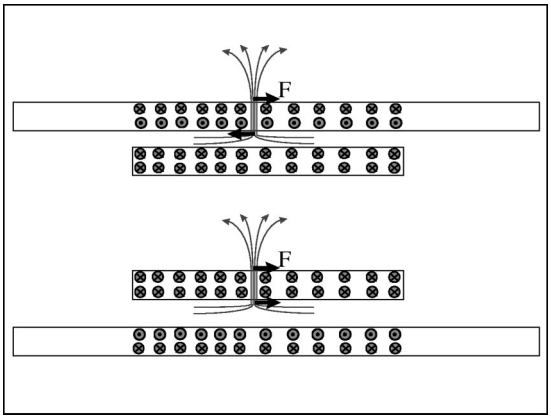

FIG. 6. Forces on a vortex in the top film when the applied current is in the bottom film (top cartoon) and bottom film (bottom cartoon).

depin the vortex. In contrast, only 2.1 and -1.5 mA applied through the top film was required to depin the same vortex. Hence, it takes roughly a factor of ten times less current through the top film than the bottom film to depin the vortex. These values are temperature dependent, as shown in Fig. 5, but the relative values are similar at all temperatures.

The second pinning site studied is located at $(0.65, -0.10)$. Vortices pinned here were obtained both by field cooling nucleation and as products of current depinning from other pinning sites. A vortex at this position did not thermally depin until 8.503 K, at which point the vortex left the junction region all together. The results of fifteen current-depinning experiments performed on vortices with the initial position of $(0.65,-0.10)$ are very similar to the results shown in Fig. 5 so they will not be shown here. At a $T_{\rm push} = 8.474$ K, 22.0 and -18.5 mA applied through the bottom film was required to depin the vortex. In contrast, only 2.0 and -1.5 mA applied through the top film was required to depin the same vortex. This characteristic was found for all four pinning sites at all temperatures at which comparative-current-depinning measurements could be obtained.

To understand the cause of this asymmetry, the applied currents and induced currents in the films must be examined.[10] If the transport current and the vortex are in the top film as shown by the bottom diagram of Fig. 6, then current flows in the same direction on both the top and bottom surfaces of the top film. As a result, the forces on the vortex from the currents in the top and bottom surfaces are in the same direction as illustrated by the bottom diagram of Fig. 6 (which looks down the long axis of the top film). If, however, the transport current is in the bottom film and the vortex is in the top film, as illustrated by the top diagram in Fig. 6 (which looks down the long axis of the botton film), then the induced Meissner current in the top film with the vortex will wrap around the film. This gives a Lorentz force to the right on the top surface and a force to the left on the bottom surface as shown. Depinning from these two different force configurations might be expected to be different.

It should be pointed out that for the current-depinning experiments with the vortices in the top Nb film, the current was applied while the bottom Nb film was normal for temperatures above 8.264 K. The current distribution in the bottom film is different depending on whether the film is superconducting or normal, but the magnetic field generated within the junction region will be nearly the same. Hence, the induced currents in the top Nb film will change only slightly when the bottom film goes normal.

The temperature dependence of the elementary pinning force f_p was measured for the pinning site located at $(0.65, -0.10)$ by applying negative current through the top film. The nucleation current was larger than the depinning current for current in the top film down to 8.043 K, with results similar to those reported earlier for Pb.[3] This allowed the top film depinning current to be measured from 8.043 to 8.503 K where the vortex spontaneously depins with no Lorentz force. Figure 7 shows the temperature dependence of the elementary pinning force in the temperature region it could be measured. At a reduced temperature of 0.95 the pinning force is 1.1×10^{-13} N or 2.75×10^{-7} N/m if the force is assumed to be uniform along the length of the vortex. This is an order of magnitude smaller than Lorentz force depinning measurements on Nb thin films by Allen and Claassen.[11] Above and below T_c of the bottom Nb film, f_p goes roughly as $(1-T/T_c)^n$ where $n=3/2$ as shown in Fig. 7. Similar values of n were also obtained from Lorentz-force depinning

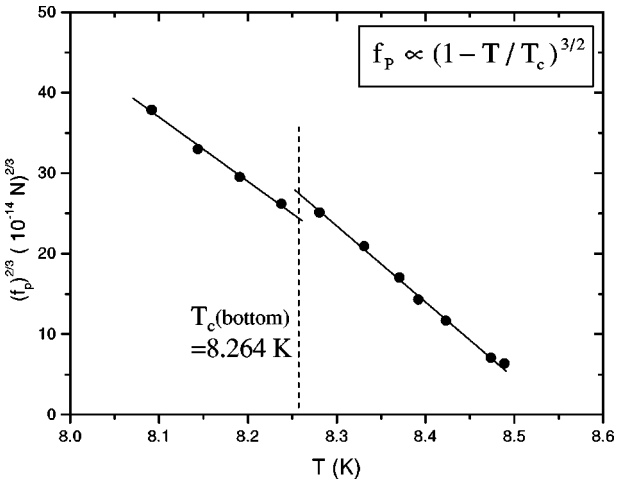

FIG. 7. Temperature dependence of the elementary pinning force f_p for a vortex pinned at $(0.65,-0.10)$ in the top Nb film.

measurements on single vortices in Nb thin films ranging from $n=1.9$ (Ref. 12) to $n=3.5$.[11] A discontinuity in f_p appears near T_c of the bottom Nb film in the junction region, 8.244 K. Above this temperature the vortex is no longer bent into the normal region of the junction by the superconductivity of the bottom Nb film and extends outward in a continuous manner. Hence, above T_c of the bottom Nb film, surface currents may interact slightly less with the magnetic field of the vortex resulting in an apparent shift in f_p.

IV. CONCLUSIONS

Artificial pinning centers were induced in the top Nb film of a Josephson junction by placing two Fe balls on top of an already characterized junction. Vortices tended to locate at the site of these Fe balls. The magnetic moments of the Fe balls were strong enough to nucleate and pin vortices beneath them even in zero applied field. The location of the induced pinning sites determined by the diffraction-pattern method were in agreement with SEM measurements of the locations of the Fe balls. For the first time the locations of artificial pinning sites for a single vortex were determined by the diffraction-pattern method and were verified by SEM measurements.

The injection of normal electrons from a line of Au into the Nb strip did not produce pinning sites as strong as the naturally occurring pinning in the Nb film. Two Josephson junctions were fabricated on substrates having 2 μm wide Au lines adjacent to the Nb layer in an attempt to depress the order parameter in the bottom Nb films and create pinning sites. For both junctions the locations of the pinning sites observed in the bottom Nb films were mapped out and compared to the locations of the Au lines determined by SEM measurements. The pinning sites were not preferentially located above the Au lines. The proximity effect from the Au line making contact with the bottom Nb film was not strong enough to pin vortices.

A large difference was found between the current in the bottom film needed to depin a vortex in the top film and current in the top film needed to depin this same vortex. For these vortices the depinning current was approximately ten times smaller for applied currents in the top film than in the bottom film. The explanation may lie in the fact that the induced currents produce a couplelike force on the vortex whereas the direct currents push in the same direction all along the vortex. At a reduced temperature of 0.95 the elementary pinning force on a vortex pinned in the top Nb film was 1.1×10^{-13} N or 2.75×10^{-7} N/m. The temperature dependence of this pinning force was approximately $(1-T/T_c)^{3/2}$ near T_c of the top Nb film.

ACKNOWLEDGMENTS

Howard Shanks of the Microelectronics Research Center provided the Si substrates with an array of Au lines. Work at Ames Laboratory was supported by the U.S. Department of Energy (DOE), Office of Basic Energy Sciences and the Office of Energy Efficiency and Renewable Energy under Contract No. W-7405-ENG-82.

[1] S.C. Sanders, J. Sok, D.K. Finnemore, and Qiang Li, Phys. Rev. B **47**, 8996 (1993).
[2] S.L. Miller, K.R. Biagi, J.R. Clem, and D.K. Finnemore, Phys. Rev. B **31**, 2684 (1985).
[3] O.B. Hyun, D.K. Finnemore, L.A. Schwartzkopf, and J.R. Clem, Phys. Rev. Lett. **58**, 599 (1987).
[4] O.B. Hyun, J.R. Clem, and D.K. Finnemore, Phys. Rev. B **58**, 599 (1989).
[5] Q. Li and D.K. Finnemore, IEEE Trans. Magn. **27**, 2913 (1991).
[6] Q. Li, J.R. Clem, and D.K. Finnemore, Phys. Rev. B **43**, 12 843 (1991).
[7] J. Sok and D.K. Finnemore, Phys. Rev. B **50**, 12 770 (1994).
[8] D. Kouzoudis, M. Breitwisch, and D.K. Finnemore, Phys. Rev. B **60**, 10 508 (1999).
[9] T.H. Alden and J.D. Livingston, J. Appl. Phys. **34**, 3551 (1966).
[10] J.R. Clem (private communication).
[11] L.H. Allen and J.H. Claassen, Phys. Rev. B **39**, 2054 (1989).
[12] G.S. Park, C.E. Cunningham, B. Cabrera, and M.E. Huber, Phys. Rev. Lett. **68**, 1920 (1992).